

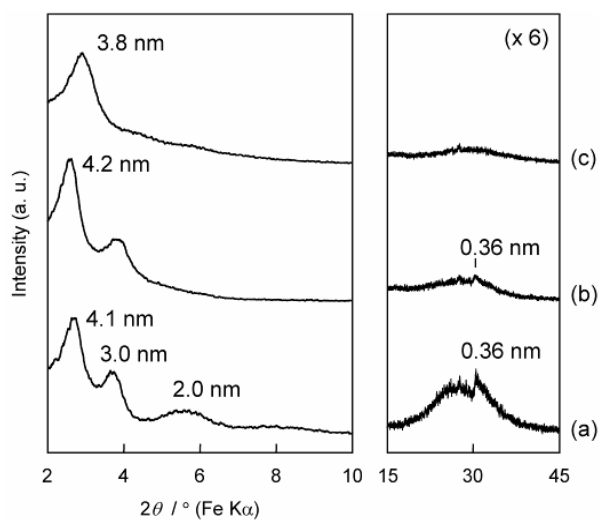
Supporting Information

Properties of Metal Species in Square-Shape Mesopores of KSW-2-Based Silica

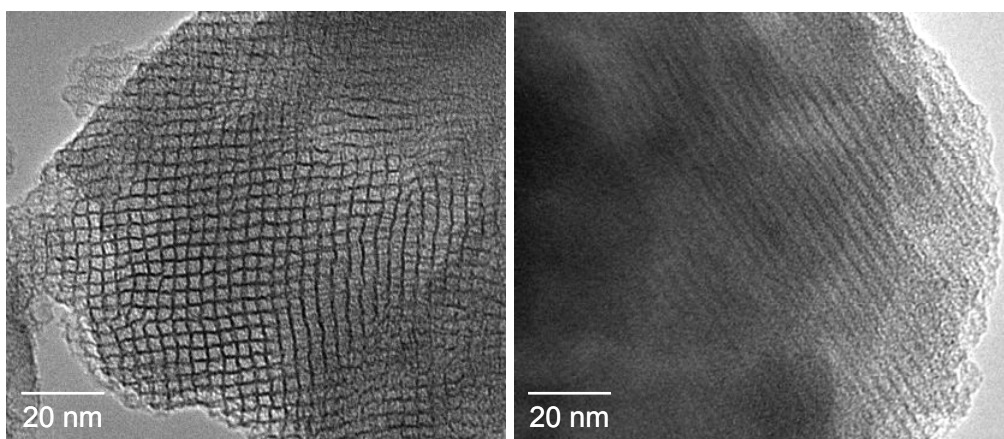
Tatsuo Kimura,* Shengjum Huang, Atsushi Fukuoka, and Kazuyuki Kuroda

Silylation of as-synthesized KSW-2 with $C_8C_1SiCl_2$

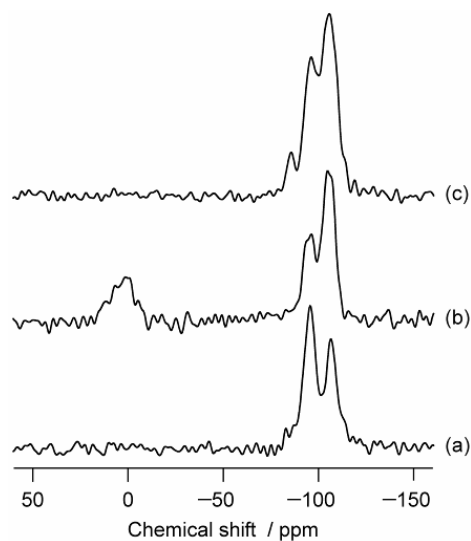
As-synthesized KSW-2, in which $C_{16}TMA$ ions were contained, was directly modified with $C_8C_1SiCl_2$ to stabilize the molecular ordering originating from kanemite, according to the previous paper.¹⁵ In the XRD pattern of as-synthesized KSW-2, the peaks with the d -spacings of 4.1, 3.0, and 2.0 nm are assignable to (11), (20), and (22) peaks due to a 2-D orthorhombic mesostructure ($c2mm$), respectively (Fig. S1a). The TEM images of as-synthesized KSW-2 also support the formation of 1-D square-shape mesopores (Fig. S2). The peak with the d -spacing of 0.36 nm is associated with the presence of a molecular ordering due to the framework of kanemite, as proved by the detailed TEM observation reported previously.¹⁶ The XRD peaks were retained after silylation with $C_8C_1SiCl_2$, but slightly broadened (Fig. S1b), being related to the presence of a new molecular ordering accumulated from the kanemite-based silicate framework. The peak with the d -spacing of 0.36 nm was hardly observed after calcination of the silylated product (Fig. S1c). The peaks due to Q^n ($n = 2-4$) species were well resolved in the ^{29}Si MAS NMR spectrum of the calcined product (Fig. S3c), suggesting that the environment of SiO_4 species in the framework was relatively identical, as well as those in the frameworks of as-synthesized KSW-2 and the silylated product (Figs. S3a and b). In addition, the width of the Q^n peaks was narrower than those observed for calcined KSW-2 without silylation (Fig. S4). The Q^3 species in as-synthesized KSW-2 are mostly considered as SiO_4 species in the original molecular ordering and reacted with $C_8C_1SiCl_2$, and then the amount of Q^4 species are increased by the addition of D^n ($n = 1, 2$) units by silylation ($D^n/Q^n = 0.31$). Finally, Q^n ($n = 2-4$) species are reformed by calcination of the silylated product to remove all the organic groups.



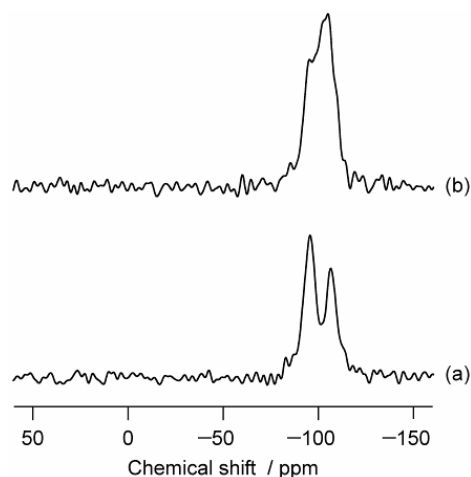
Supporting Fig S1. XRD patterns of (a) as-synthesized KSW-2, (b) the product silylated with $C_8C_1SiCl_2$, and (c) the calcined product.



Supporting Fig S2. TEM images of as-synthesized KSW-2.



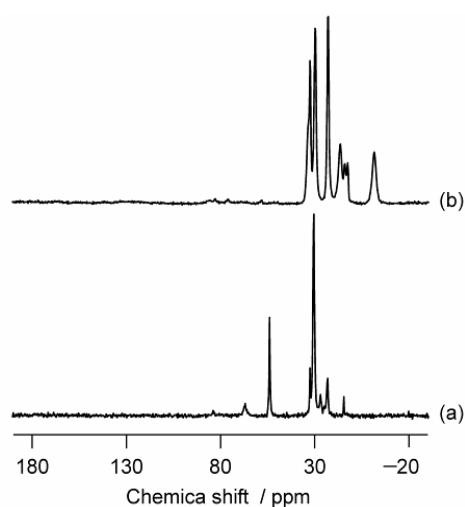
Supporting Fig S3. ^{29}Si MAS NMR spectra of (a) as-synthesized KSW-2, (b) the product silylated with $\text{C}_8\text{C}_1\text{SiCl}_2$, and (c) the calcined product.



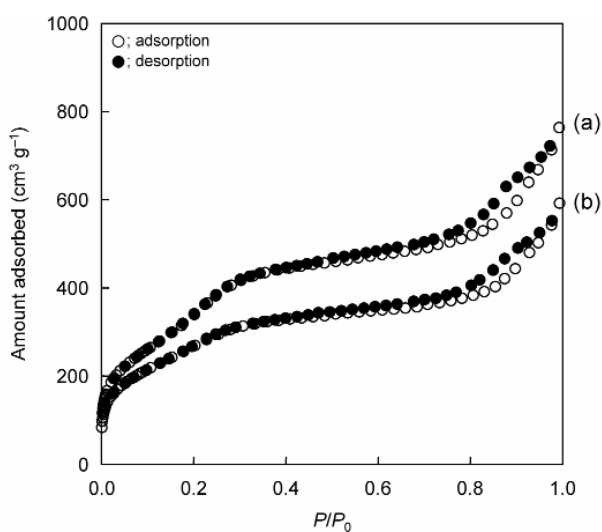
Supporting Fig S4. ^{29}Si MAS NMR spectra of (a) as-synthesized KSW-2 and (b) the calcined product without silylation.

The ^{13}C CP/MAS NMR spectra of as-synthesized KSW-2 and the silylated product are shown in Fig. S5. Only the peaks due to carbon atoms in attached organosilyl groups were observed without any peaks due to carbon atoms of C_{16}TMA ions after silylation. The result indicates that C_{16}TMA ions are eliminated during silylation, which is also supported by CHN analysis. Both nitrogen (2.1 mass %) and carbon atoms (35.0 mass %) due to C_{16}TMA ions (C/N ratio = 19.4) were detected in as-synthesized KSW-2, while nitrogen atoms were hardly detected after silylation (< 0.1 mass %). Therefore, all the carbon atoms (27.5 mass %) in the silylated product are considered to

come from octyl and methyl groups. The N_2 adsorption-desorption isotherms of the calcined products of as-synthesized KSW-2 and the silylated product are shown in Fig. S6. Both of the isotherms showed type IV behaviors, as observed typically for ordered mesoporous silicas. The BET surface area (S_{BET}), the pore volume (V_{total}), and the pore diameter ($4V_{0.8}/S$) of Si-KSW-2 (silylated and then calcined) were smaller than those of calcined KSW-2 (Table 1) because the silicate surfaces of square-shape mesopores were covered with new siloxane networks.

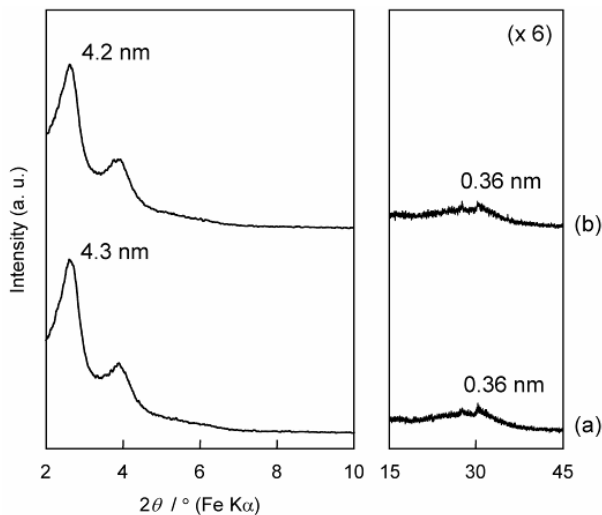


Supporting Fig S5. ^{13}C CP/MAS NMR spectra of (a) as-synthesized KSW-2 and (b) the product silylated with $C_8C_1SiCl_2$.

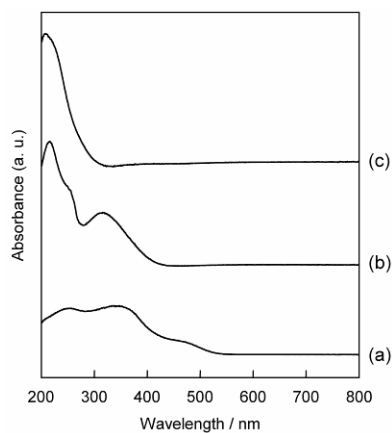


Supporting Fig S6. N_2 adsorption-desorption isotherms of the calcined products of (a) as-synthesized KSW-2 and (b) the KSW-2 silylated with $C_8C_1SiCl_2$.

Characterization of titanium grafted KSW-2-based mesoporous silica



Supporting Fig S7. XRD patterns of the products silylated with $\text{C}_8\text{C}_1\text{SiCl}_2$ in the presence of (a) Cp_2TiCl_2 and (b) CpTiCl_3 ($\text{Si}/\text{Ti} = 250$).



Supporting Fig S8. UV-Vis spectra of (a) CpTiCl_3 diluted with MgCO_3 , (b) the product silylated with $\text{C}_8\text{C}_1\text{SiCl}_2$ in the presence of CpTiCl_3 ($\text{Si}/\text{Ti} = 250$), and (c) the calcined product.